

**Cell type dependent changes in CdSe/ZnS quantum dot uptake and toxic endpoints**

Journal:	<i>Toxicological Sciences</i>
Manuscript ID:	TOXSCI-14-0750.R1
Manuscript Type:	Research Article
Date Submitted by the Author:	29-Nov-2014
Complete List of Authors:	Manshian, Bella; KU Leuven, Molecular Imaging; Swansea University, College of Medicine Soenen, Stefaan; KU Leuven, Medicine Al-Ali, Abdullah; Swansea University, College of Medicine Wills, John; Swansea University, Engineering Hondow, Nicola; University of Leeds, Engineering Brown, Andy; University of Leeds, Engineering Jenkins, Gareth; Swansea University, College of Medicine Doak, Shareen; Swansea University, College of Medicine
Key Words:	Cell type, Cellular uptake, Nanoparticles , Quantum dots, Cytotoxicity , Genotoxicity < Genetic Toxicology
Society of Toxicology Specialty Section Subject Area:	Nanotoxicology [121]

**Cell type dependent changes in CdSe/ZnS quantum dot uptake and toxic endpoints**

*Bella B. Manshian,<sup>†‡</sup> Stefaan J. Soenen,<sup>‡</sup> Abdullah Al-Ali,<sup>†</sup> Andy Brown,<sup>§</sup> Nicole Hondow,<sup>§</sup>  
John Wills,<sup>†</sup> Gareth J.S. Jenkins,<sup>†</sup> Shareen H. Doak.\**

<sup>†</sup>Institute of Life Science, College of Medicine, Swansea University, Singleton Park, Swansea SA2 8PP, UK; <sup>‡</sup>Biomedical NMR unit-MoSAIC, Department of Medicine, KU Leuven, B-3000 Leuven, Belgium; <sup>§</sup>Institute for Materials Research, SCaPE, University of Leeds, Leeds LS2 9JT, UK.

\*\*To whom correspondence should be addressed at Swansea University, Institute of Life Science, College of Medicine, Singleton Park, Swansea SA2 8PP, UK. Fax: 0044 1792 295388. Email: [s.h.doak@swansea.ac.uk](mailto:s.h.doak@swansea.ac.uk).

**Abstract**

Toxicity of nanoparticles (NPs) is often correlated with the physicochemical characteristics of the materials. However, some discrepancies are noted in in-vitro studies on quantum dots (QD) with similar physicochemical properties. This is partly related to variations in cell type. In this study we show that epithelial (BEAS-2B), fibroblast (HFF-1) and lymphoblastoid (TK6) cells show different biological responses following exposure to QDs. These cells represented the three main portals of NP exposure; bronchial, skin, and circulatory. The uptake and toxicity of negatively and positively charged CdSe:ZnS QDs of the same core size but with different surface chemistries (carboxyl or amine polymer coatings) were investigated in full and reduced serum containing media following 1 and 3 cell cycles. Following thorough physicochemical characterisation, cellular uptake, cytotoxicity and gross chromosomal damage were measured. Cellular damage mechanisms in the form of reactive oxygen species and the expression of inflammatory cytokines IL8 and TNF $\alpha$  were assessed. QDs uptake and toxicity significantly varied in the different cell lines. BEAS-2B cells demonstrated the highest level of QDs uptake yet displayed a strong resilience with minimal genotoxicity following exposure to these NPs. In contrast, HFF-1 and TK6 cells were more susceptible to toxicity and genotoxicity respectively as a result of exposure to QDs. Thus, this study demonstrates that in addition to nanomaterial physicochemical characterisation, a clear understanding of cell type dependent variation in uptake coupled to the inherently different capacities of the cell types to cope with exposure to these exogenous materials are all required to predict genotoxicity.

**Keywords:** Cell type, Cellular uptake, Nanoparticle, Quantum dots, Cytotoxicity, Genotoxicity.

## Introduction

Photoluminescent, nanoparticulate, semiconductor quantum dots (QDs) have great potential for electronic, medical and biological applications; they are proving to be particularly promising advanced imaging tools at the molecular and diagnostic level (Bagalkot *et al.*, 2007; Chen *et al.*, 2010; Fu *et al.*, 2009; Peng *et al.*, 2012; Wu *et al.*, 2003; Yang *et al.*, 2009). However, with increasingly widespread manufacture and use comes the risk of increased human and environmental exposure to, in some cases, significant numbers of these particles (Oberdorster *et al.*, 2005). When used in biomedical applications these materials will likely be introduced into patients however disposal of consumer products containing QDs may also result in their release into the environment at high local concentrations, where they might accumulate and degrade (Kahru and Ivask, 2013; Scheringer, 2008). Our current knowledge of the potential health effects of exposure to QDs is mainly derived from acute cytotoxicity studies, and the data generated suggest that QDs may exert adverse effects in the skin (Zhang *et al.*, 2008), lungs (Geys *et al.*, 2008; Jacobsen *et al.*, 2009), gastrointestinal tract (Wang *et al.*, 2008) and other tissues (Soenen *et al.*, 2012; Tang *et al.*, 2008). The debate surrounding the potential toxicity of QDs still persists; for instance, no toxicity could be found in a pilot study on non-human primates (Ye *et al.*, 2012). Yet, it has been suggested that QDs are not excreted efficiently, thus, exposure could potentially lead to long term health problems (Sealy, 2012). Furthermore, several studies have reported problems in correlating *in-vitro* to *in-vivo* findings thus more factors, such as NP dosing should be considered (Tsoi *et al.*, 2013; Yong *et al.*, 2013). It is also becoming increasingly apparent that any observed biological findings must be carefully correlated with the physicochemical properties of the QDs, as the many variations in chemical composition, structure, coating agents and sizes

1  
2  
3 make it very hard to derive general conclusions on toxicity (Singh *et al.*, 2009; Ye, *et al.*,  
4  
5 2012).  
6

7  
8 Amongst recent findings the intrinsic ability of different cells to take up and process  
9  
10 nanomaterials differently, thus potentially resulting in varying toxicity profiles, has been  
11  
12 receiving increased attention. Although some studies have shown that CdSe/ZnS QDs can  
13  
14 cause cytotoxic damage at specific exposure concentrations (Soenen, *et al.*, 2012), whether  
15  
16 this is true for all cell types remains an area of limited understanding. There are a small  
17  
18 number of studies indicating that QDs do have some capacity for inducing DNA damage (Aye  
19  
20 *et al.*, 2013; Choi *et al.*, 2012; Ju *et al.*, 2013), however, often the cell lines used in these  
21  
22 studies were cancer-derived that may be more resistant or sensitive to DNA damage and  
23  
24 therefore may not be wholly representative of the *in-vivo* situation. Thus, to reduce the gap  
25  
26 between *in-vitro* and *in-vivo* studies and to provide a better understanding of the toxicity  
27  
28 results reported in *in-vitro* studies more research is needed to highlight the role of different  
29  
30 cell types in governing the uptake and consequent potential genotoxicity following exposure  
31  
32 to QDs. Furthermore, it has been shown that serum content in exposure media can affect NP  
33  
34 uptake and hence mask the genotoxic potential of a class of NPs (Doak *et al.*, 2009) and this  
35  
36 may be a confounding factor in many of the current QD reports. Another aspect that has been  
37  
38 missed in previous studies is the role of time in the observed toxicity which has often has been  
39  
40 limited to a maximum of 24h. Thus, there is opportunity for investigations that systematically  
41  
42 examine the genotoxic potential of QDs by associating uptake and DNA damage capacity  
43  
44 with cell type whilst accounting for exposure times and varying serum conditions.  
45  
46  
47  
48  
49

50  
51 The aim of the present study was therefore to investigate variability in uptake and  
52  
53 genotoxicity in three human cell lines with varying tissues of origin following exposure to  
54  
55 QDs with different surface chemistries. The use of two QDs with similar chemical  
56  
57 composition but coated with different functional groups (carboxyl versus amine) enabled  
58  
59  
60

1  
2  
3 additional consideration of the role of QDs surface functionalization in cellular uptake, cyto-  
4 and geno-toxicity. Where cyto- and/or geno-toxicity was observed, underlying mechanisms  
5 were investigated, including the generation of reactive oxygen species (ROS), expression of  
6 inflammatory cytokines IL8 and TNF $\alpha$ , changes in mitochondrial membrane potential (MMP)  
7 and classification of DNA damage as aneugenic and/or clastogenic. This multiparametric  
8 approach allowed for an improved understanding of the role of the cell type in the observed  
9 genotoxic effects, particularly taking into consideration varying cellular growth characteristics  
10 as BEAS-2B and HFF-1 are adherent cells, while TK6 are suspension cells.  
11  
12  
13  
14  
15  
16  
17  
18  
19  
20  
21  
22  
23

## 24 **Materials and Methods**

### 25 **Cell culture**

26  
27  
28  
29 Human lymphoblastoid-B TK6 suspension cells, human bronchial epithelial BEAS-2B cells  
30 and human foreskin fibroblast HFF-1 cell lines were applied in this study. All cell lines were  
31 purchased from ATCC (ATCC Cell lines Service, USA) and were maintained in 75cm<sup>2</sup> flasks  
32 at a concentration of 1.5x10<sup>5</sup> cells/ml. TK6 cells were cultured in Rosewell Park Memorial  
33 Institute (RPMI-1640) medium supplemented with 1% 2mM L-Glutamine (Gibco<sup>®</sup>, UK), and  
34 10% horse serum (Gibco<sup>®</sup>, UK). BEAS-2B cells were propagated in Dulbecco's Modified  
35 Eagle's Medium (DMEM) in the presence of 10% foetal bovine serum (FBS; Gibco<sup>®</sup>, UK).  
36 HFF-1 cells required DMEM medium supplemented with 15% FBS. All cells were incubated  
37 in an atmosphere of 37°C and 5% CO<sub>2</sub>. For all the experiments cells were seeded at 1.5x10<sup>5</sup>  
38 cells/ml in culture medium containing reduced or full serum and allowed to settle overnight  
39 prior to treatment with 0, 2.5, 5, 7.5, 10, 15, and 20nM dispersions of QDs for 1 or 3 cell  
40 cycles. These concentrations were selected according to the OECD guidelines which states  
41 that at least four concentrations which should cover a range of high toxicity to little or no  
42  
43  
44  
45  
46  
47  
48  
49  
50  
51  
52  
53  
54  
55  
56  
57  
58  
59  
60

1  
2  
3 toxicity should be used (Doak *et al.*, 2012). The highest concentration was selected based on  
4  
5 previous results by Soenen et al. (Soenen *et al.*, 2012). Experiments conducted at 2 cell cycles  
6  
7 did not reveal significant differences to the 1 cell cycle results (data not shown).  
8  
9

### 10 11 12 13 **Quantum dot nanoparticles**

14  
15  
16 CdSe/ZnS core/shell fluorescent nanocrystals with amine- (Cytodiagnostics, Canada), and  
17  
18 carboxyl- (Invitrogen, UK) functional ligands attached to the surface were used. The average  
19  
20 diameter of each QD including its core and shell was 4-10 nm according to the manufacturer's  
21  
22 notes. The emission maxima of each QD were 585 and 665nm for the carboxyl- and amine-  
23  
24 QDs respectively. Prior to cell exposure, carboxyl- and amine-QDs were suspended in water  
25  
26 and vortexed for 30 seconds immediately prior to introduction into the cell cultures. The  
27  
28 reduced serum concentration selected was based on optimization studies to identify the lowest  
29  
30 serum content that could be applied for the experimental duration without altering cell growth  
31  
32 parameters (data not presented). BEAS-2B and HFF-1 cells tolerated 2% serum while TK6  
33  
34 cells accepted 1% serum conditions. Cells were exposed to QDs for 1 or 3 cell cycles, where  
35  
36 one cell cycle corresponded to 18hr for TK6 cells, and 24 hr for both BEAS-2B and HFF-1  
37  
38 cells.  
39  
40  
41  
42  
43  
44  
45  
46  
47

### 48 **Physicochemical characterisation studies**

49  
50 The hydrodynamic diameter, obtained by dynamic light scattering (DLS), and the zeta  
51  
52 potential of the QDs were measured with a Malvern 4700 system (Malvern instruments  
53  
54 Limited, UK) at 15nM in water, RPMI-1640 medium with and without 1% or 10% horse  
55  
56  
57  
58  
59  
60

1  
2  
3 serum, and DMEM with or without 2%, 10% and 15% fetal bovine serum at 37 °C. Data are  
4  
5 presented as the average of 30 readings (10 readings per replicate).  
6  
7

8 The QDs were prepared for TEM by placing a drop of suspended QDs onto a copper grid  
9  
10 coated with a holey carbon support film (Agar Scientific Ltd) and plunge frozen in liquid  
11  
12 ethane followed by freeze drying preserving the original features of the QDs (Hondow *et al.*,  
13  
14 2012). Images were subsequently captured. Images were collected by an FEI Tecnai TF20  
15  
16 FEG-TEM operating at 200 kV fitted with a Gatan Orius SC600A camera and an Oxford  
17  
18 Instruments INCA 350 EDX system with an 80 mm<sup>2</sup> X-Max SDD detector.  
19  
20  
21  
22  
23  
24

## 25 26 **Cellular uptake studies**

### 27 28 *ImageStream analysis*

29  
30  
31  
32 Treated cells were harvested and FACS fixed (BD Biosciences, UK) for 30 min at room  
33  
34 temperature. Samples were passed through the ImageStream imaging flow cytometer (Amnis  
35  
36 Corporation) and fluorescence was measured at 488 nm and 633 nm. All experiments were  
37  
38 conducted in duplicate and 5000 cells were acquired for each replicate. Data were analysed  
39  
40 using the Ideas v5 software (Amnis Corporation).  
41  
42  
43  
44  
45  
46

### 47 48 *Transmission Electron Microscopy*

49  
50 For cellular uptake studies, samples were prepared as previously described (Hondow *et al.*,  
51  
52 2011). Briefly, the treated cells were harvested and placed in 2.5% glutaraldehyde fixative.  
53  
54 Thin sections (~70 nm) were cut from the polymerised block using an ultra-microtome (Leica  
55  
56 Microsystems, EM UC7). TEM microscopy was conducted as previously described (Hondow,  
57  
58  
59  
60

1  
2  
3 *et al.*, 2011) on a FEI Tecnai F20 operating at 200 kV and fitted with a GatanOrius SC600A  
4  
5 CCD camera for imaging and an Oxford Instruments X-Max SD detector for energy  
6  
7 dispersive X-ray (EDX) analysis.  
8  
9

### 10 11 12 13 14 **pH effect on QD stability**

15  
16  
17 The effect of different pH levels on the fluorescence of these NPs was also investigated. QDs  
18  
19 were incubated in 10% HS mixed with PBS and pH levels were adjusted to 7.4, 5.5, and 4.5.  
20  
21 Particle suspensions were prepared at 2.5, 5, 5.5, 10, 15nM and 20nM concentrations in 100µl  
22  
23 total volume. Particles were incubated with the different media in black 96 well plates  
24  
25 (Greiner Bio One BVBA, Belgium). All experiments were accompanied by a negative control  
26  
27 and were conducted in triplicates. Fluorescence measurements were taken using the Omega  
28  
29 multiwell plate reader (BMG Labtech, Belgium) on days 1, 2, 3, 4, and 5 post preparation.  
30  
31  
32  
33  
34  
35  
36

### 37 **Cell viability assay**

38  
39  
40 Cytotoxicity induced by exposure of the two QD types in BEAS-2B, HFF-1, and TK6 cell  
41  
42 lines were determined according to their relative population doubling (RPD) as previously  
43  
44 described (Singh *et al.*, 2012). All experiments were performed in duplicate with solvent-only  
45  
46 negative controls and mitomycin-C (MMC) at 0.01 µg/ml was used as a positive control. Cell  
47  
48 viability was considered significantly decreased when percent relative population doubling  
49  
50 was less than or equal to 50% (according to the OECD guidelines).  
51  
52  
53  
54  
55  
56

### 57 **Cytokinesis blocked micronucleus assay**

58  
59  
60

1  
2  
3 Gross chromosomal damage was quantified with the cytokinesis blocked micronucleus  
4 (CBMN) assay, performed as previously described (Manshian *et al.*, 2013a) using a post-  
5 treatment cytochalasin-B protocol where cells were incubated for 24 h in full serum  
6 containing medium supplemented with 3 µg /ml cytochalasin B following treatment with QDs  
7 for 1 or 3 cell cycles. All experiments were performed in duplicate and mitomycin-C (MMC)  
8 at 0.01 µg/ml was used as a positive control. Harvested cells were stained with 4',6-  
9 diamidino-2-phenylindole (DAPI) and scanned on the Metafer automated scoring image  
10 analysis system (MetaSystems, Carl Zeiss Ltd). The frequency of micronuclei in 3000  
11 binucleated cells per replicate was determined. As each concentration was performed in  
12 duplicate, the micronucleus frequency in 6000 binucleated cells in total per exposure  
13 concentration was assessed, which represents substantially enhanced sensitivity and statistical  
14 power over routine analysis which only requires scoring of 2000 cells per exposure  
15 concentration; OECD TG487.  
16  
17  
18  
19  
20  
21  
22  
23  
24  
25  
26  
27  
28  
29  
30  
31  
32  
33  
34  
35

### 36 **Pan centromeric staining**

37  
38  
39 Slides prepared for the micronucleus assay were used for pancentromeric staining, however  
40 cells were fixed in 95% methanol for 10min. Fluorescent in situ hybridisation (FISH) was  
41 performed using a human pan centromeric probe labelled with FITC (Cambio, UK) and slides  
42 were analysed under a Zeiss fluorescent microscope (Carl Zeiss, UK) at x63 magnification.  
43  
44  
45  
46  
47 The presence of a centromeric signal was assessed in 100 micronuclei (50 per replicate)  
48 present in binucleated cells. Micronuclei containing a fluorescence signal were classified as  
49 centromere positive containing a whole chromosome (aneugenic); while those lacking a  
50 fluorescently labelled region were centromere negative and therefore contained chromosome  
51 fragments (clastogenic).  
52  
53  
54  
55  
56  
57  
58  
59  
60

### ROS and MMP analysis

ROS levels and MMP experiments were conducted in TK6 and HFF-1 cells as previously described (Soenen *et al.*, 2013). Briefly,  $2 \times 10^5$  cells/ml were seeded in black 96 well plates (Greiner Bio One, UK) and allowed to settle for 1 cell cycle after which they were treated with the QDs dispersed at 0, 2.5, 5, 7.5, 10, 15, and 20nM concentrations for 4 or 24 h. Each experiment was conducted in triplicate and was accompanied with controls treated similarly but without addition of detection reagent or with QDs and reagent in the absence of cells verifying the induction of ROS in the cells due to the QDs and lack of QD interference with the ROS assay. All experiments were accompanied with positive control treatments of 0.33M (1%)  $H_2O_2$  for 2 h prior to incubation with 10  $\mu$ M 5-(and-6)-chloromethyl-2',7'-dichlorodihydrofluorescein diacetate, acetyl ester (CM-H<sub>2</sub>DCFDA; Molecular Probes, Invitrogen, UK) or 20  $\mu$ M JC-10 (Enzo Life Sciences, UK) for ROS and MMP experiments respectively. Cells were washed twice with PBS and analysed under an Omega microplate reader (BMG Labtech, UK) at 480 nm excitation with 540 nm emission (ROS analysis) or 520nm and 590 nm emission (MMP assessment) according to the manufacturer's recommendations. For MMP experiments, the data obtained were expressed as the proportion of damaged over healthy mitochondria (green/red).

### Enzyme linked immunosorbent assay (ELISA)

TK6 and HFF-1 cells were seeded into T25 culture flasks at  $1.5 \times 10^5$  cells/ml in 10 ml total culture medium containing reduced and full serum. Following overnight incubation cells were treated with the QDs for 1 cell cycle, then the supernatant was collected and ELISA assays

1  
2  
3 (IL8: Human CXCL8/IL-8 DuoSet; and TNF- $\alpha$ : Human TNF-alpha DuoSet; R&D Systems,  
4 Abingdon, UK) were performed as per the supplier's guidelines. All experiments were  
5 conducted in triplicate.  
6  
7  
8  
9

### 10 11 12 **Statistical analysis**

13  
14  
15  
16 All data are expressed as the mean  $\pm$  standard deviation (SD). ImageStream results are  
17 represented as fluorescence intensity levels relative to untreated control cells and are  
18 expressed as the mean  $\pm$  standard error of the mean. Micronucleus frequency was examined  
19 for significance with the Fisher's exact test, while ROS, MMP, and ELISA results were  
20 analysed using one-way ANOVA.  
21  
22  
23  
24  
25  
26  
27  
28  
29

### 30 **Results**

#### 31 32 **Characterisation of QD physicochemical properties**

33  
34  
35  
36 Quantum dot size distribution, morphology, crystallinity, zeta potential and agglomeration  
37 status were investigated as a part of the physico-chemical characterisation study.  
38  
39

40  
41 TEM analyses on the QDs in their primary-as purchased- state demonstrated that amine-QDs  
42 were generally 3-5 nm in diameter (**Table 1**), with evidence of crystallinity seen at higher  
43 magnifications while carboxyl-QDs were spherical and approximately 4-5 nm in diameter.  
44  
45  
46  
47

48  
49 The hydrodynamic diameter for the QDs in the various solutions (**Table 1**) representing the  
50 size range of agglomerates in the serum containing media revealed that the amine-QDs  
51 formed larger agglomerates than the carboxyl-QDs (**Table 1**). Additionally, a clear variation  
52 in agglomerate size was noticeable between reduced and full serum conditions, where the  
53 QDs formed smaller agglomerates in full serum (FBS or HS) compared to reduced serum.  
54  
55  
56  
57  
58  
59  
60

1  
2  
3 Overall, zeta potential measurements mainly revealed a low negative surface charge in the  
4 various dispersion media tested, indicating the potential for the absence of colloidal stability  
5 (Table 1). Amine QDs demonstrated a slightly higher positive zeta-potential in water and in  
6 DMEM but this was near the neutral range. As anticipated, carboxyl-QDs showed a higher  
7 negative charge in water which was masked in the presence of media containing serum.  
8  
9  
10  
11  
12  
13  
14  
15  
16  
17

### 18 **Cellular uptake**

19  
20  
21 Three, well established, genetically stable mammalian cells, TK6, BEAS-2B, and HFF-1,  
22 were used to examine QD uptake. Two image based techniques were employed to investigate  
23 this parameter. ImageStream imaging flow cytometry and TEM. Quantitative measurements  
24 were attained from the analysis of ImageStream images. This approach allowed the  
25 quantitation of QD uptake which was coupled to direct identification and sub-cellular  
26 localisation by TEM image analysis.  
27  
28  
29  
30  
31  
32  
33  
34  
35  
36  
37  
38

### 39 ***ImageStream flow cytometry***

40  
41  
42 Clear differences in relative intra-cellular fluorescence intensity were seen between the three  
43 cell lines exposed to each of the test QDs (Figure 1). In general, fluorescence intensity, hence  
44 uptake levels, were much higher in BEAS-2B and TK6 cells compared to the HFF-1 cells. For  
45 BEAS-2B cells, clear concentration-dependent uptake could be seen for both amine- and  
46 carboxyl-QDs, where this was not the case for HFF-1 cells. Carboxylated QDs demonstrated  
47 higher uptake than amine-QDs. For example, in BEAS-2B cells exposed to 15nM of  
48 carboxyl-QDs, relative fluorescence intensity values of over 3000% were obtained, compared  
49 to 1100% for BEAS-2B cells exposed to an equivalent concentration of amine-QDs in full  
50  
51  
52  
53  
54  
55  
56  
57  
58  
59  
60

1  
2  
3 serum conditions. Carboxyl-QDs were readily taken up by all three cell lines with the highest  
4 uptake seen in BEAS-2B followed by TK6 and then HFF-1 cells. In TK6 cells this  
5 corresponded to a 2900-fold increase in cellular fluorescence in 1% serum conditions  
6 compared to the controls. Uptake of the same QDs was much less in 10% serum conditions  
7 (only 400-fold). No significant uptake was noted in these cells when exposed to the amine-  
8 QD. For both QDs serum conditions (reduced versus full) did not play a major role in cellular  
9 uptake levels except for TK6 cells exposed to carboxyl-QDs where significantly lower uptake  
10 was observed in full serum compared to reduced serum containing media (a ~ 20 fold drop of  
11 intensity between reduced and full serum) (**Figure 1C**). Uptake levels in HFF-1 cells were  
12 substantially lower than the other two cell types and were not significantly different from  
13 negative controls except following exposure to carboxyl-QDs, which were significantly  
14 internalised at 7.5nM and 15nM concentrations in full and reduced serum conditions (**Figure**  
15 **1A**). Thus, the order of increasing cellular uptake based on cell line and QD surface coating  
16 type were BEAS-2B > TK6 > HFF-1 and carboxyl- > amine-QDs, respectively.  
17  
18  
19  
20  
21  
22  
23  
24  
25  
26  
27  
28  
29  
30  
31  
32  
33  
34  
35  
36  
37

### 38 *Transmission electron microscopy (TEM)*

39  
40  
41 Defining ultimate sub-cellular localisation of nanoparticles inside cells can only truly be  
42 achieved by TEM and thus, this technique was subsequently employed to ascertain the  
43 positioning of QDs inside the test cells. TEM images of BEAS-2B, TK6, and HFF-1 cells  
44 revealed the presence of carboxyl-QDs in all three cell types (**Figure 2a, d and j**). Amine-  
45 QDs were also identified within BEAS-2B (**Figure 2g**) and HFF-1 cells (**Figure 2m**). With  
46 respect to the carboxyl- and amine-QDs, in some instances (e.g. **Figure 2m**) large collections  
47 of QDs could be identified at low magnifications, however in all cases higher magnification  
48 imaging and elemental spectroscopy were undertaken to both confirm the presence of the QDs  
49  
50  
51  
52  
53  
54  
55  
56  
57  
58  
59  
60

1  
2  
3 and also to determine the intracellular location (**Figure 2b, e, h, k and n**). The QDs could be  
4 found either free in the cytoplasmic space or localised in intracellular vesicles which appeared  
5 to be endosomes or lysosomes. TEM images suggested amine-QDs were present in larger  
6 agglomerates in vesicles within HFF-1 cells (**Figure 2n**) compared to those in the BEAS-2B  
7 cells (**Figure 2h**). Similarly, more carboxyl-QDs were detected in BEAS-2B cells (**Figure 2e**)  
8 followed by TK6 (**Figure 2b**) and HFF-1 cells (**Figure 2k**) respectively, which correlates  
9 with the ImageStream data presented in Figure 1.  
10  
11  
12  
13  
14  
15  
16  
17  
18

19 Cadmium was detected in all EDX analyses (**Figure 2c, f, , l and o**), confirming the  
20 nanoparticulate features imaged were internalised QDs and not a sample preparation feature  
21 (e.g. from the osmium tetroxide fixative) or an artefact (e.g. signals due to the cellular  
22 environment, such as calcium). Elements from the TEM support grid itself (e.g. copper and  
23 carbon) were also evident in the EDX spectra.  
24  
25  
26  
27  
28  
29  
30  
31  
32  
33

### 34 **pH effect on QD degradation**

35  
36 The two QD particles were incubated with media adjusted to different pH levels (7.4, 5.5, 4.5)  
37 for 1, 2, 3, 4, and 5 days and fluorescence intensity were analysed. These experiments were  
38 conducted at 0, 2.5, 5, 7.5, 10, 15, and 20 nM concentrations, however, the graph shown here  
39 presents only data for the 7.5nM dose for the purpose of conciseness. Results revealed a sharp  
40 decline in fluorescence intensity with carboxyl QDs starting at Day1 in all three pH media  
41 (**Figure 3A**). Some decline in fluorescence was detected in the amine QDs (**Figure 3B**),  
42 however, this was not significant at any time point.  
43  
44  
45  
46  
47  
48  
49  
50  
51  
52  
53  
54  
55

### 56 **Cytotoxic effects of QDs**

57  
58  
59  
60

1  
2  
3 Results of the RPD analysis revealed that no significant cytotoxicity was observed in BEAS-  
4  
5 2B cells exposed to carboxyl- or amine-QDs in the presence of 2% or 10% serum after 1 or 3  
6  
7 cell cycles (**Figure 4C, 4D**). Exposing HFF-1 cells to carboxyl-QDs in full (15%) serum  
8  
9 containing media for 1 cell cycle induced notable cytotoxicity, which increased following 3  
10  
11 cell cycle exposures with significantly decreased cell viability (down to  $\leq 38.5\%$ ) at  
12  
13 concentrations  $\geq 7.5\text{nM}$ . This was however not the case in reduced serum experiments where  
14  
15 no toxicity was observed (**Figure 4A, 4B**). TK6 and HFF-1 cells suffered high levels of  
16  
17 toxicity at concentrations higher than 15nM (data not shown on graph) whilst BEAS-2B cells  
18  
19 were able to tolerate concentrations of up to 20nM (**Figures 4C and 4D**).  
20  
21  
22  
23  
24  
25  
26

### 27 **QD Genotoxicity**

28  
29  
30 Chromosomal damage was analysed by the cytokinesis blocked micronucleus assay, with  
31  
32 micronuclei (MN) scored in a minimum of 6000 binucleated cells per exposure concentration  
33  
34 to enhance sensitivity of the test system. Of the two types of QDs examined, only the  
35  
36 carboxyl-QD induced chromosomal damage in full serum containing media. The carboxyl-  
37  
38 QDs resulted in a significant increase in MN frequency at several exposure concentrations in  
39  
40 both TK6 and HFF-1 cells after 1 cell cycle exposures (**Figure 5**). Prolonged exposure to  
41  
42 carboxyl-QDs for 3 cell cycles in TK6 cells resulted in an increase in MN induction (**Figure**  
43  
44 **5F**). HFF-1 cells showed a concentration dependent increase in MN following exposure to  
45  
46 amine-QDs up to 10nM in media with reduced serum (**Figure 5A**). No MN were detected in  
47  
48 BEAS-2B cells exposed to either of the QDs (**Figure 5C, 5D**). Therefore, no further analyses  
49  
50 were conducted on these cell types due to the absence of any significant cyto- and geno-toxic  
51  
52 effects.  
53  
54  
55  
56  
57  
58  
59  
60

### QD genotoxicity mechanisms

The mechanisms underlying the cyto- and geno-toxic effects of the QDs were subsequently examined, focusing on the nature of the DNA damage, the effect of oxidative stress and secondary mechanisms such as mitochondrial membrane potential ( $\Delta\psi_m$ ).

Pan-centromeric staining was utilised to determine whether the gross chromosomal damage induced by the QDs was caused by clastogenic or aneugenic events. These experiments were conducted in both TK6 and HFF-1 cells in both full and reduced serum containing media. In TK6 cells amine-QDs showed a concentration-dependent trend of increasing aneuploidy (ranging from 50% to 76% MN containing whole chromosomes) induced in both 1% and 10% serum containing media (**Figure 6**). This effect was less pronounced with the carboxyl-QDs. In HFF-1 cells pan-centromeric detection was only performed in full serum conditions due to the absence of sufficient micronuclei in the reduced serum conditions. Interestingly, in this cell line both QDs induced mainly clastogenic events (**Figure 6C**).

The production of ROS was investigated due to its association with toxicity following exposure to certain NPs. However, only minimal cytoplasmic ROS was detected, mainly in HFF-1 cells exposed to the carboxyl-QD and TK6 cells exposed to amine-QDs (**Figure 7**). With respect to mitochondrial membrane permeability, no observable effects were seen in HFF-1 or TK6 cells exposed to any QDs in full serum conditions (**Figure 8**). In contrast, a significant and concentration dependent increase in MMP was recorded in TK6 and HFF-1 cells treated with carboxyl-QDs in reduced serum containing media. This increase in MMP occurred after 4 h and 24 h treatments in TK6 and HFF-1 cells respectively (**Figure 8 B, D**).

The potential inflammatory effects of the QDs were also evaluated by determining the release of either IL-8 or TNF- $\alpha$  by TK6, BEAS-2B or HFF-1 cells when exposed to amine- or carboxyl-QDs by means of specific ELISA assays. The cells were exposed to the QDs for 24

1  
2  
3 h over a broad concentration range (0, 2.5, 5, 7.5, 10 or 15 nM), but no increase in the level of  
4  
5 excreted IL-8 or TNF- $\alpha$  could be observed for any QD type at any concentration compared  
6  
7 with the level produced by untreated control cells (data not shown). These results were limited  
8  
9 to the two cytokines investigated in this work which is not conclusive of the inflammatory  
10  
11 state of these cell lines following exposure to the QDs in this study.  
12  
13

## 14 15 16 17 **Discussion**

18  
19 The HFF-1, BEAS-2B and TK6 cell lines are considered important targets for NP toxicity  
20  
21 studies (Lai *et al.*, 2008; Li *et al.*, 2012; Nymark *et al.*, 2012) because they represent three  
22  
23 major ports of exposure to NPs. However, the present investigation demonstrates that when  
24  
25 exposed to the same NPs, each of these cells demonstrate clear differences in subsequent  
26  
27 genotoxicity profiles. This could partly be related to the different tissue source of these cell  
28  
29 lines being epithelial, fibroblast and lymphoblastoid. The consequences of QD exposure were  
30  
31 tested in full serum and reduced serum conditions, following acute and extended exposure  
32  
33 durations to examine the role of cellular repair in overriding any observed damage.  
34  
35 Nonetheless, QD toxicity was found to be highly dependent on the cell type under  
36  
37 investigation.  
38  
39  
40  
41

42 Carboxyl- and amine-QDs with a similar core size, demonstrating a variable degree of  
43  
44 agglomeration according to their surface chemistry, were used. Amine-QDs were found to  
45  
46 agglomerate most extensively, whereas the carboxyl-QD agglomerates were relatively  
47  
48 smaller. The degree of agglomeration also depended largely on the nature of the cell culture  
49  
50 media and the amount of serum present. These differences in agglomeration appear to have  
51  
52 led to significant variation in the resultant cellular interactions. The carboxyl-QDs formed the  
53  
54 smallest agglomerates, and produced the most pronounced uptake levels in all three cell types.  
55  
56  
57  
58  
59  
60

1  
2  
3 With respect to cellular uptake, imaging flow cytometry revealed that BEAS-2B cells  
4 exhibited the highest levels of QD internalization, followed by TK6 cells and then HFF-1  
5 cells. Considering that quantifying fluorescence levels in the intracellular environment has its  
6 challenges as intracellular pH level alterations can affect their fluorescence quantum yield,  
7 thus, we examined the role of different pH levels on the QDs used. Our results showed that  
8 though changes in pH levels resulted in degradation in carboxyl and not amine QDs but this  
9 did not affect its fluorescence intensity. However, it was clear from these analyses that  
10 carboxyl QDs had a much higher innate fluorescence compared to amine NPs. For example,  
11 the fluorescence intensity of 7.5nM carboxyl QDs in pH 7.4 on day 1 was 259810 compared  
12 to 51061 in its amine counterpart at the same conditions. Even though there is a 5 fold  
13 difference in these values however this effect is not what we see in the ImageStream uptake  
14 results. Thus, the difference in cellular uptake stems from a combination of interrelated  
15 factors being the higher initial brightness of the carboxyl QDs yet the reduced fluorescence  
16 intensity of these QDs in intracellular conditions, and differences in the cellular capacity for  
17 QD internalization. Moreover, even though the different cells had a different propagation  
18 time (18hr for TK6 and 24 hr for the BEAS-2B and HFF-1 cells) but this difference was not  
19 big enough to be accounted for the difference noted in the cellular uptake. For example, in a  
20 study investigating proliferation of TK6 cells only 20% of the cells were found in G2/M phase  
21 following 6 hr (Ren *et al.*, 2011) and in another study TK6 cells were evidenced to start the  
22 first doubling after 16 hr (Noonan *et al.*, 2012). Although cellular uptake was observed with  
23 all three cell lines after 1 cell cycle this did not always result in significant cyto- or geno-  
24 toxicity.  
25  
26  
27  
28  
29  
30  
31  
32  
33  
34  
35  
36  
37  
38  
39  
40  
41  
42  
43  
44  
45  
46  
47  
48  
49  
50

51  
52 This study demonstrated that uptake levels do not always correlate with the presence of  
53 toxicity since BEAS-2B cells demonstrated the highest level of uptake for both amine- and  
54 carboxyl-QDs yet they were most resistant to cyto- or genotoxic effects. The TK6 cells  
55  
56  
57  
58  
59  
60

1  
2  
3 appeared to be the most sensitive, especially given the lower level of cell-associated QDs,  
4  
5 indicating the cells were unable to tolerate even low levels of internalised QDs. The high  
6  
7 internalisation of carboxyl-QDs also resulted in the greatest induction of genotoxicity,  
8  
9 oxidative stress and mitochondrial damage all of which were found to show concentration-  
10  
11 dependent relationships. All particles demonstrated clear toxicological differences depending  
12  
13 on the presence of low or high serum conditions, which may be attributed to serum protein  
14  
15 corona on the QDs affecting interactions between the QDs and the cellular membrane leading  
16  
17 to alterations in the rate of internalisation and in their intracellular effects.  
18  
19

20  
21 Despite BEAS-2B proving to be the most resistant cell following exposure to QDs, in other  
22  
23 studies, the same cells have shown some susceptibility to cytotoxicity. This is true for  
24  
25 polystyrene NP where there was more obvious damage induced in BEAS-2B compared to  
26  
27 macrophage, epithelial and cancer cell lines (Xia *et al.*, 2008). Similarly, significant levels of  
28  
29 chromosomal damage have been previously reported when BEAS-2B cells were exposed to  
30  
31 single walled carbon nanotubes (Manshian *et al.*, 2013b).  
32  
33

34  
35 Differences in cellular response to QD exposure could partly be due to the mechanisms by  
36  
37 which they impart cellular stress. Thus, to further understand the implications of QD exposure  
38  
39 the generation of ROS was explored given its important role in toxicity generated from NPs  
40  
41 and specifically QD exposure (Lewinski *et al.*, 2008; Soenen, *et al.*, 2012). However, no  
42  
43 significant induction of ROS was detected in any of the treatments here. These observations  
44  
45 are different to ones previously reported by Soenen *et al.* (Soenen, *et al.*, 2012) where ROS  
46  
47 induction was found for up to 20nM exposure concentration to the same commercially  
48  
49 available carboxyl-QDs as applied in the present investigation. This difference could be due  
50  
51 to the very different cell types used (HUVEC, PC12, and C17.2 cells), with substantial  
52  
53 differences in anti-oxidative capacity (Soenen, *et al.*, 2012). It is also plausible that the ROS  
54  
55 generated in these cells were not detectable with the assays used in this study. It is well  
56  
57  
58  
59  
60

1  
2  
3 known that quantitative analysis of ROS can often be hindered by the intracellular presence of  
4 high levels of thiyl or sulfinyl radicals formed by glutathione which along with other agents  
5 can lead to the scavenging of ROS (Cossarizza *et al.*, 2009). Although genotoxic effects were  
6 seen in the TK6 cells following exposure to QDs, the limited induction of ROS in TK6 cells  
7 correlates with the fact that largely aneugenic responses were detected (as oxidative stress  
8 typically induces clastogenicity) (Emerit *et al.*, 2000). Thus, the intrinsic homeostatic  
9 differences in varying cell types could be of particular importance in understanding the  
10 potential toxicity imparted by specific NMs.  
11  
12  
13  
14  
15  
16  
17  
18  
19

20  
21 Other factors that were determined to play a role in QD induced toxicity in this study included  
22 QD surface charge, exposure media composition and serum content, plus the exposure  
23 duration. For example, here, HFF-1 cells demonstrated no cytotoxicity following exposure to  
24 amine-QDs; yet significant cell death was observed at high concentrations when the cells  
25 were exposed to carboxyl-QDs for 3 cell cycles. When genotoxicity was considered, the  
26 carboxyl-QDs did not impart any chromosomal damage in the HFF-1 cells, while amine-QDs  
27 induced a significant induction of micronuclei after 1 cell cycle which was absent following 3  
28 cell cycles. This NP dependent toxicity difference therefore highlights the importance of  
29 considering the physicochemical characteristics as well as other factors in such studies. Not  
30 only was this apparent when genotoxicity was considered, but was also responsible for  
31 different mechanistic processes underlying the cellular damage. For instance, carboxyl-QDs  
32 induced a significant concentration dependent increase in MMP, while amine-QDs did not  
33 appear to cause any such change. These effects were only detected in reduced serum condition  
34 in both HFF-1 and TK6 cells. Consequently, this could suggest a role for the protein corona  
35 which might influence the uptake mechanics of these NPs (Monopoli *et al.*, 2012). It is well  
36 known that NPs bind to serum proteins at different extents depending on their surface charge.  
37  
38  
39  
40  
41  
42  
43  
44  
45  
46  
47  
48  
49  
50  
51  
52  
53  
54  
55  
56  
57  
58  
59  
60 In two recent studies negatively charged gold and iron oxide NPs bound more strongly to

1  
2  
3 plasma proteins eliciting different biological responses to their positively charged  
4 counterparts (Deng *et al.*, 2013; Sakulku *et al.*, 2014). These findings might therefore  
5 explain our results where in general carboxyl QDs were more readily taken up in reduced  
6 serum conditions compared to full serum media resulting in more pronounced cytotoxic and  
7 genotoxic consequences in these conditions.  
8  
9

10  
11  
12  
13  
14 In conclusion, QD induced cyto- and geno-toxicity are strongly affected by a multitude of  
15 parameters including: 1) differences in cell type potentially resulting in varying surface area  
16 contact with the exposed material, in addition to inherent cellular differences in internalising  
17 NPs and ability to cope with an exogenous insult; 2) the nature of the QD surface chemistry;  
18  
19 3) the degree of QD agglomeration in the presence of varying amounts of serum proteins; 4)  
20 differences in cell culture media composition; and 5) time of exposure. We suggest that these  
21 factors influence the degree of agglomeration and sedimentation of the particles that  
22 subsequently influence the level and nature of cell-association. The latter translates itself in  
23 differences in cyto- and geno-toxicity that do not always directly correlate with the quantity of  
24 internalised material, but are also strongly influenced by the intrinsic cellular capacity for  
25 handling internalised foreign material, which is cell type dependent.  
26  
27  
28  
29  
30  
31  
32  
33  
34  
35  
36  
37  
38

39  
40 Thus, it is pertinent that future studies follow multiparametric approaches for studying NP  
41 induced toxicity. Of particular importance is the consideration of multiple target organ  
42 specific cell types in parallel to obtain a more complete understanding of the biological  
43 consequences of a specific nanomaterial exposure.  
44  
45  
46  
47  
48  
49  
50  
51  
52

### 53 **Acknowledgements**

54  
55 We would like to thank the Engineering and Physical Sciences Research Council (EPSRC) for  
56 the funding that supported this research (grant application number EP/H008683/1). Stefaan J  
57  
58  
59  
60

1  
2  
3 Soenen is a postdoctoral fellow of the FWO-Vlaanderen. Additionally we wish to  
4  
5 acknowledge the generous financial support provided to Mr. Abdullah Al-Ali by the State of  
6  
7 Kuwait Ministry of Defence, which supported his contribution to this research.  
8  
9

### 10 11 12 13 **Declaration of Interest**

14  
15  
16  
17 The authors declare that they have no competing interests.  
18  
19  
20  
21  
22  
23  
24  
25  
26  
27  
28  
29  
30  
31  
32  
33  
34  
35  
36  
37  
38  
39  
40  
41  
42  
43  
44  
45  
46  
47  
48  
49  
50  
51  
52  
53  
54  
55  
56  
57  
58  
59  
60

**References**

- 1  
2  
3  
4  
5 Aye, M., et al. (2013). Genotoxic and mutagenic effects of lipid-coated CdSe/ZnS quantum dots. *Mutat*  
6  
7  
8 *Res* **750**(1-2), 129-38.  
9  
10  
11 Bagalkot, V., et al. (2007). Quantum dot-aptamer conjugates for synchronous cancer imaging, therapy,  
12  
13 and sensing of drug delivery based on bi-fluorescence resonance energy transfer. *Nano letters* **7**(10),  
14  
15 3065-70.  
16  
17  
18 Chen, L., et al. (2010). Quantum-dots-based fluoroimmunoassay for the rapid and sensitive detection of  
19  
20 avian influenza virus subtype H5N1. *Luminescence : the journal of biological and chemical*  
21  
22 *luminescence* **25**(6), 419-23.  
23  
24  
25 Choi, Y. J., et al. (2012). Cyto-/genotoxic effect of CdSe/ZnS quantum dots in human lung  
26  
27 adenocarcinoma cells for potential photodynamic UV therapy applications. *J Nanosci Nanotechnol*  
28  
29 **12**(3), 2160-8.  
30  
31  
32 Cossarizza, A., et al. (2009). Simultaneous analysis of reactive oxygen species and reduced glutathione  
33  
34 content in living cells by polychromatic flow cytometry. *Nature protocols* **4**(12), 1790-7.  
35  
36  
37 Deng, Z. J., et al. (2013). Plasma protein binding of positively and negatively charged polymer-coated  
38  
39 gold nanoparticles elicits different biological responses. *Nanotoxicology* **7**(3), 314-22.  
40  
41  
42 Doak, S. H., et al. (2009). Confounding experimental considerations in nanogenotoxicology.  
43  
44 *Mutagenesis* **24**(4), 285-93.  
45  
46  
47 Doak, S. H., et al. (2012). In vitro genotoxicity testing strategy for nanomaterials and the adaptation of  
48  
49 current OECD guidelines. *Mutat Res* **745**(1-2), 104-11, 10.1016/j.mrgentox.2011.09.013.  
50  
51  
52 Emerit, I., et al. (2000). Clastogenic factors as biomarkers of oxidative stress in chronic hepatitis C.  
53  
54 *Digestion* **62**(2-3), 200-7, 7814.  
55  
56  
57 Fu, X., et al. (2009). A robust and fast bacteria counting method using CdSe/ZnS core/shell quantum  
58  
59 dots as labels. *Journal of microbiological methods* **79**(3), 367-70.  
60

- 1  
2 Geys, J., et al. (2008). Acute Toxicity and Prothrombotic Effects of Quantum Dots: Impact of Surface  
3 Charge. *Environ Health Persp* **116**(12), 1607-1613.  
4  
5  
6  
7 Hondow, N., et al. (2011). STEM mode in the SEM: a practical tool for nanotoxicology.  
8  
9 *Nanotoxicology* **5**(2), 215-27.  
10  
11 Hondow, N., et al. (2012). Quantitative characterization of nanoparticle agglomeration within  
12 biological media. *J Nanopart Res* **14**(7), Artn 977.  
13  
14  
15  
16  
17 Jacobsen, N. R., et al. (2009). Lung inflammation and genotoxicity following pulmonary exposure to  
18 nanoparticles in ApoE(-/-) mice. *Part Fibre Toxicol* **6**, Artn 2.  
19  
20  
21  
22  
23 Ju, L., et al. (2013). Quantum dot-related genotoxicity perturbation can be attenuated by PEG  
24 encapsulation. *Mutat Res* **753**(1), 54-64.  
25  
26  
27  
28 Kahru, A., and Ivask, A. (2013). Mapping the dawn of nanoecotoxicological research. *Acc Chem Res*  
29  
30 **46**(3), 823-33.  
31  
32  
33 Lai, J. C., et al. (2008). Exposure to titanium dioxide and other metallic oxide nanoparticles induces  
34 cytotoxicity on human neural cells and fibroblasts. *Int J Nanomedicine* **3**(4), 533-45.  
35  
36  
37 Lewinski, N., et al. (2008). Cytotoxicity of nanoparticles. *Small* **4**(1), 26-49.  
38  
39  
40 Li, Y., et al. (2012). Genotoxicity of silver nanoparticles evaluated using the Ames test and in vitro  
41 micronucleus assay. *Mutat Res* **745**(1-2), 4-10.  
42  
43  
44  
45  
46 Manshian, B. B., et al. (2013a). The in vitro micronucleus assay and kinetochore staining: methodology  
47 and criteria for the accurate assessment of genotoxicity and cytotoxicity. *Methods in molecular biology*  
48  
49 **1044**, 269-89.  
50  
51  
52  
53 Manshian, B. B., et al. (2013b). Single-walled carbon nanotubes: differential genotoxic potential  
54 associated with physico-chemical properties. *Nanotoxicology* **7**(2), 144-56.  
55  
56  
57  
58  
59  
60

1  
2 Monopoli, M. P., et al. (2012). Biomolecular coronas provide the biological identity of nanosized  
3 materials. *Nature nanotechnology* 7(12), 779-86.  
4  
5

6  
7 Noonan, E. M., et al. (2012). O6-Methylguanine DNA lesions induce an intra-S-phase arrest from  
8 which cells exit into apoptosis governed by early and late multi-pathway signaling network activation.  
9  
10 Integrative biology : quantitative biosciences from nano to macro 4(10), 1237-55.  
11  
12

13  
14 Nymark, P., et al. (2012). Genotoxicity of polyvinylpyrrolidone-coated silver nanoparticles in BEAS  
15 2B cells. *Toxicology*, S0300-483X(12)00369-1.  
16  
17

18  
19 Oberdorster, G., et al. (2005). Nanotoxicology: An emerging discipline evolving from studies of  
20 ultrafine particles. *Environ Health Persp* 113(7), 823-839.  
21  
22

23  
24 Peng, C. W., et al. (2012). Quantum-dots based simultaneous detection of multiple biomarkers of tumor  
25 stromal features to predict clinical outcomes in gastric cancer. *Biomaterials* 33(23), 5742-52.  
26  
27

28  
29 Ren, X., et al. (2011). Comparison of proliferation and genomic instability responses to WRN silencing  
30 in hematopoietic HL60 and TK6 cells. *PloS one* 6(1), e14546, 10.1371/journal.pone.0014546.  
31  
32

33  
34 Sakulkhu, U., et al. (2014). Protein Corona Composition of Superparamagnetic Iron Oxide  
35 Nanoparticles with Various Physico-Chemical Properties and Coatings. *Sci Rep-Uk* 4, Artn 5020.  
36  
37

38  
39 Scheringer, M. (2008). Nanoecotoxicology: Environmental risks of nanomaterials. *Nature*  
40 *nanotechnology* 3(6), 322-3.  
41  
42

43  
44 Sealy, C. (2012). Primates show mixed response to quantum dots. *Nano Today* 7(4), 223-224.  
45

46  
47 Singh, N., et al. (2009). NanoGenotoxicology: the DNA damaging potential of engineered  
48 nanomaterials. *Biomaterials* 30(23-24), 3891-914.  
49  
50

51  
52 Singh, N., et al. (2012). The role of iron redox state in the genotoxicity of ultrafine superparamagnetic  
53 iron oxide nanoparticles. *Biomaterials* 33(1), 163-70.  
54  
55

56  
57 Soenen, S. J., et al. (2012). The cytotoxic effects of polymer-coated quantum dots and restrictions for  
58 live cell applications. *Biomaterials* 33(19), 4882-8.  
59  
60

- 1  
2 Soenen, S. J., et al. (2013). Fluorescent non-porous silica nanoparticles for long-term cell monitoring:  
3 cytotoxicity and particle functionality. *Acta biomaterialia* **9**(11), 9183-93.  
4  
5  
6 Tang, M. L., et al. (2008). Mechanisms of unmodified CdSe quantum dot-induced elevation of  
7 cytoplasmic calcium levels in primary cultures of rat hippocampal neurons. *Biomaterials* **29**(33), 4383-  
8 4391.  
9  
10  
11  
12  
13 Tsoi, K. M., et al. (2013). Are quantum dots toxic? Exploring the discrepancy between cell culture and  
14 animal studies. *Acc Chem Res* **46**(3), 662-71.  
15  
16  
17  
18 Wang, L., et al. (2008). Toxicity of CdSe Nanoparticles in Caco-2 Cell Cultures. *Journal of*  
19 *Nanobiotechnology* **6**, 11.  
20  
21  
22  
23 Wu, X. Y., et al. (2003). Immunofluorescent labeling of cancer marker Her2 and other cellular targets  
24 with semiconductor quantum dots (vol 21, pg 41, 2003). *Nat Biotechnol* **21**(4), 452-452.  
25  
26  
27  
28 Xia, T., et al. (2008). Cationic polystyrene nanosphere toxicity depends on cell-specific endocytic and  
29 mitochondrial injury pathways. *ACS nano* **2**(1), 85-96.  
30  
31  
32  
33 Yang, L., et al. (2009). Single chain epidermal growth factor receptor antibody conjugated  
34 nanoparticles for in vivo tumor targeting and imaging. *Small* **5**(2), 235-43.  
35  
36  
37  
38 Ye, L., et al. (2012). A pilot study in non-human primates shows no adverse response to intravenous  
39 injection of quantum dots. *Nat Nano* **7**(7), 453-458.  
40  
41  
42  
43 Yong, K.-T., et al. (2013). Nanotoxicity assessment of quantum dots: from cellular to primate studies.  
44 *Chemical Society Reviews* **42**(3), 1236-1250.  
45  
46  
47 Zhang, L. W., et al. (2008). Biological interactions of quantum dot nanoparticles in skin and in human  
48 epidermal keratinocytes. *Toxicology and applied pharmacology* **228**(2), 200-11.  
49  
50  
51  
52  
53  
54  
55  
56  
57  
58  
59  
60

## Figure Legends

**Figure 1. ImageStream cellular uptake analysis following QD exposure.** (A) HFF-1; (B) BEAS-2B; and (C) TK6 cells exposed to amine- and carboxyl-QD for 24 h in low serum or high serum containing media. Each graph is accompanied with representative results of cellular uptake images captured with ImageStream. Where appropriate, the degree of significance is indicated (\*:  $p < 0.05$ , \*\*:  $p < 0.01$ , \*\*\*:  $p < 0.001$ ).

**Figure 2. High angle annular dark field (HAADF) scanning transmission electron microscope (STEM) images confirming QDs uptake.** (a) carboxyl-QDs into TK6 cells accompanied with (b) higher magnification images of particles plus (c) assertion of particle composition by BF TEM EDX spectroscopy. No amine-QDs could be detected in TK6 cells using this technique (in line with ImageStream analysis). (d,e,f) carboxyl- and (g,h,i) amine-QDs in BEAS-2B cells and (j,k,l) carboxyl and (m,n,o) amine-QDs uptake into HFF-1 cells.

**Figure 3. Effect of pH on QDot fluorescence intensity.** Relative fluorescence intensity levels of 7.5 nM suspensions of amine and carboxyl QDs at various pH values (7.4, 5.5, 4.5) as a function of time. Data are presented as mean  $\pm$  SD. Where appropriate, the degree of significance is indicated (\*:  $p < 0.05$ , \*\*:  $p < 0.01$ , \*\*\*:  $p < 0.001$ ).

**Figure 4. Cytotoxicity induced following exposure of human cells to QDs.** (A, C, D) amine- and (B, D, E) carboxyl-QDs exposure to (A, B) HFF-1; (C, D) BEAS-2B; and (E, F) TK6 cells for 1 and 3 cell cycles exposure times in full and reduced serum containing media. Data are presented as mean  $\pm$  SD.

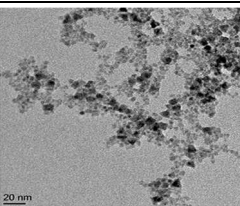
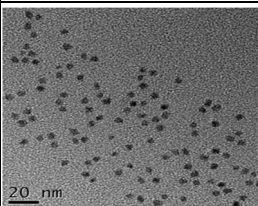
1  
2  
3  
4  
5 **Figure 5. Micronucleus induction following exposure of human cells to QDs.** (A) HFF-1, (B)  
6 BEAS-2B, and (C) TK6 cells exposed to amine- and carboxyl-QDs for 1 and 3 cell cycles time points in  
7 full and reduced serum containing media. Data are presented as mean  $\pm$  SD. The MN frequency for the  
8 0.01  $\mu$ g/ml MMC positive control was 3.08 $\pm$ 0.44%, 2.3 $\pm$ 0.45% and 5.2 $\pm$ 0.457% for TK6, HFF-1 and  
9 BEAS-2B cells respectively. Where appropriate, the degree of significance is indicated (\*:  $p < 0.05$ , \*\*:  $p < 0.01$ , \*\*\*:  $p < 0.001$ ).

10  
11  
12  
13  
14  
15  
16  
17  
18  
19  
20  
21  
22  
23 **Figure 6. Ratio of micronuclei containing whole chromosomes (centromere positive) to DNA-**  
24 **fragments (centromere negative) for TK6 cells exposed to QDs.** Pan-centromeric staining in TK6  
25 and HFF-1 cells exposed to amine- and carboxyl-QDs for 24 h in A) TK6 cells 1% serum; B) TK6  
26 cells 10% serum; and C) HFF-1 cells 15% serum containing medium. (D, E) Representative  
27 fluorescence images of a binucleated TK6 cell with (D) or without (E) a centromere positive  
28 micronucleus (indicated by white arrows). Centromere-positive and centromere-negative micronuclei  
29 were differentiated by the presence of bright yellow-green signal after pan-centromeric antibody  
30 staining (green). Nuclei were counterstained with DAPI (blue).  
31  
32  
33  
34  
35  
36  
37  
38  
39  
40  
41  
42  
43  
44  
45

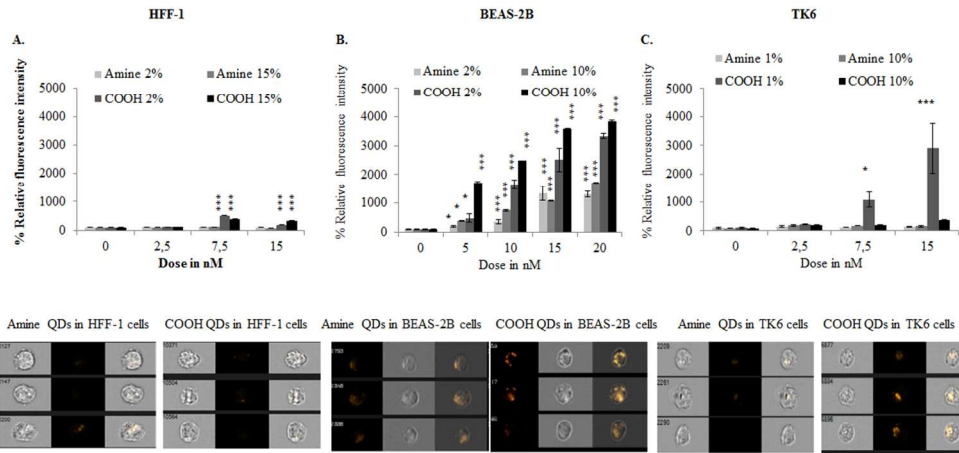
46 **Figure 7. ROS induction in TK6 and HFF-1 cells treated with;** (A, C) amine-, and (B, D) carboxyl-  
47 QDs for 4 or 24 h in full (dark grey) and reduced (light grey) serum conditions. Data are expressed as  
48 fluorescence intensity levels relative to untreated control cells and are represented as the mean  $\pm$   
49 standard error of the mean. The relative fluorescence intensity for the H<sub>2</sub>O<sub>2</sub> positive control was  
50 250 $\pm$ 50% and 200 $\pm$ 45% for the TK6 and HFF-1 exposed cells respectively. Where appropriate, the  
51 degree of significance is indicated (\*:  $p < 0.05$ , \*\*:  $p < 0.01$ , \*\*\*:  $p < 0.001$ ).

1  
2  
3  
4  
5 **Figure 8. Mitochondrial damage induced following QD exposure.** A, B) HFF-1 and C, D) TK6 cells  
6 following 4 h and 24 h exposure to A, C) amine-, B, D) carboxyl- QDs in low serum (light grey) and  
7 high serum (dark grey) conditions. Following uptake in healthy mitochondria, the green fluorescent JC-  
8 10 dye is converted into red clusters and the ratio of green over red mitochondria is used as a measure  
9 of the integrity of the mitochondria in the specific cell. Data are expressed relative to untreated control  
10 cells and are represented as the mean  $\pm$  SD. The relative fluorescence intensity for the H<sub>2</sub>O<sub>2</sub> positive  
11 control was 182 $\pm$ 22% and 130 $\pm$ 2% for the TK6 and HFF-1 exposed cells respectively. Where  
12 appropriate, the degree of significance is indicated (\*: p < 0.05, \*\*: p < 0.01, \*\*\*: p < 0.001).  
13  
14  
15  
16  
17  
18  
19  
20  
21  
22  
23  
24  
25  
26  
27  
28  
29  
30  
31  
32  
33  
34  
35  
36  
37  
38  
39  
40  
41  
42  
43  
44  
45  
46  
47  
48  
49  
50  
51  
52  
53  
54  
55  
56  
57  
58  
59  
60

**Table 1. Summary of the physico-chemical characteristics of the QDs investigated.** Surface charge, diameter according to TEM images of primary NPs, average zeta potential and hydrodynamic diameter distribution of QD agglomerates in water, RPMI or DMEM medium with reduced (1%, or 2%) and full (10%, or 15%) serum conditions is presented. DLS results are provided with their polydispersion index (PDI) values.

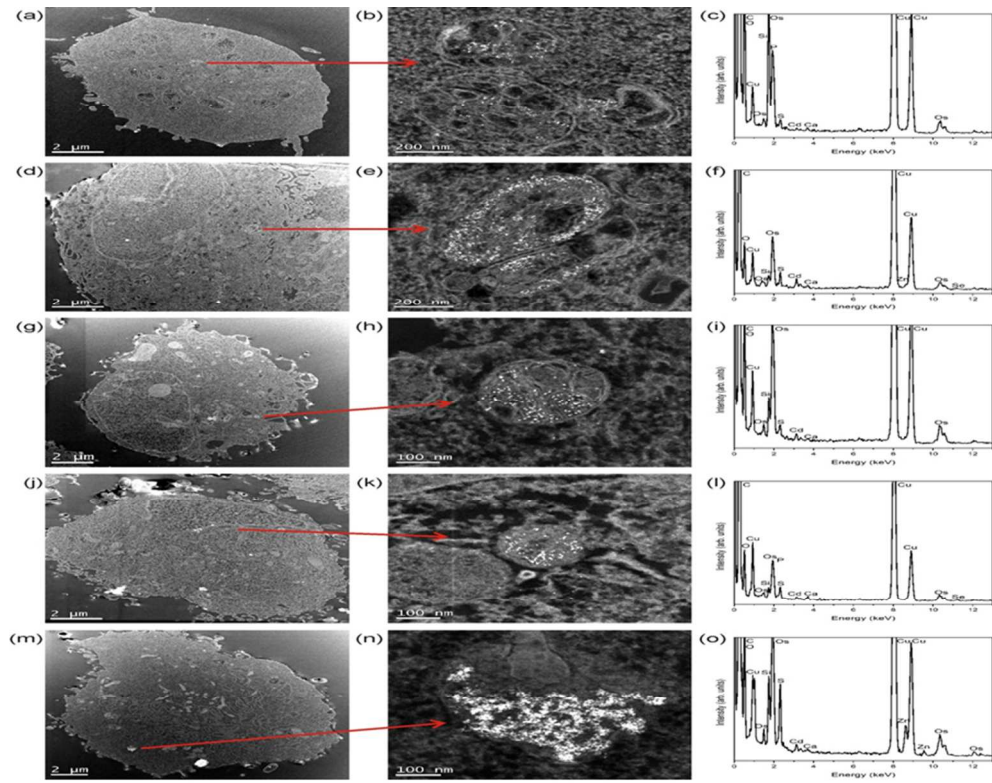
	Physico-chemical characteristics	Culture medium	QD NPs	
			Amine	Carboxyl
<b>Surface charge</b>			Positive	Negative
<b>Primary QD diameter by TEM</b>			 3-5nm	 4-5nm
<b>Water</b>	z-Potential (mV)	-13.8	8.71	-30.40
	Size range (mean size in nm)	—	295-1106 (615)	91-1106 (255)
	PDI	—	0.789	0.400
<b>RPMI 1% HS</b>	z-Potential (mV)	-5.16	-9.64	-4.79
	Size range (mean size in nm)	4,19-615 (16)	164-955 (342)	4.8-712 (13)
	PDI	0.316	1.000	0.395
<b>RPMI 10% HS</b>	z-Potential (mV)	-2.78	-10.60	-6.92
	Size range (mean size in nm)	4.2-342 (152)	58-1281 (220)	4.8-295 (11)
	PDI	0.33	0.608	0.362
<b>DMEM 2% FBS</b>	z-Potential (mV)	-11.23	5.75	-12.35
	Size range (mean size in nm)	2.7-342 (16)	58-1484 (531)	5.6-396 (15)
	PDI	0.399	0.456	0.217
<b>DMEM 10% FBS</b>	z-Potential (mV)	-6.6	+4.8	-10.6
	Size range (mean size in nm)	3.6-164 (22)	1.74-955 (42)	4.2-295.3 (19)
	PDI	0.146	0.122	0,608
<b>DMEM 15% FBS</b>	z-Potential (mV)	-7.98	4.80	-10.60
	Size range (mean size in nm)	3.62-190 (15)	37-615 (141)	3.1-190 (11)
	PDI	0.350	0.484	0.363

1  
2  
3  
4  
5  
6  
7  
8  
9  
10  
11  
12  
13  
14  
15  
16  
17  
18  
19  
20  
21  
22  
23  
24  
25  
26  
27  
28  
29  
30  
31  
32  
33  
34  
35  
36  
37  
38  
39  
40  
41  
42  
43  
44  
45  
46  
47  
48  
49  
50  
51  
52  
53  
54  
55  
56  
57  
58  
59  
60



101x47mm (300 x 300 DPI)

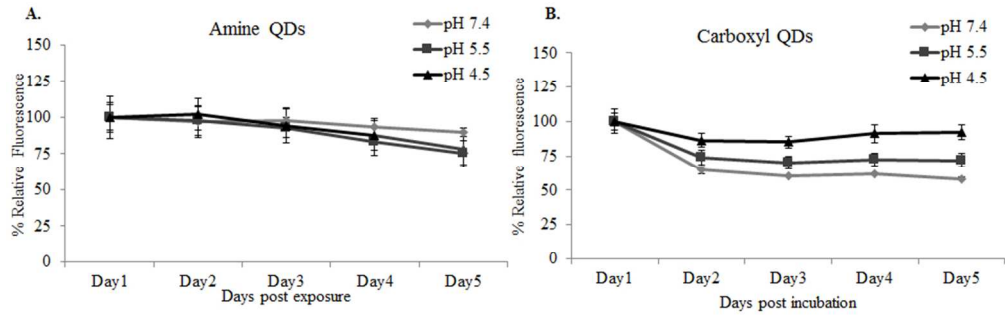
1  
2  
3  
4  
5  
6  
7  
8  
9  
10  
11  
12  
13  
14  
15  
16  
17  
18  
19  
20  
21  
22  
23  
24  
25  
26  
27  
28  
29  
30  
31  
32  
33  
34  
35  
36  
37  
38  
39  
40  
41  
42  
43  
44  
45  
46  
47  
48  
49  
50  
51  
52  
53  
54  
55  
56  
57  
58  
59  
60



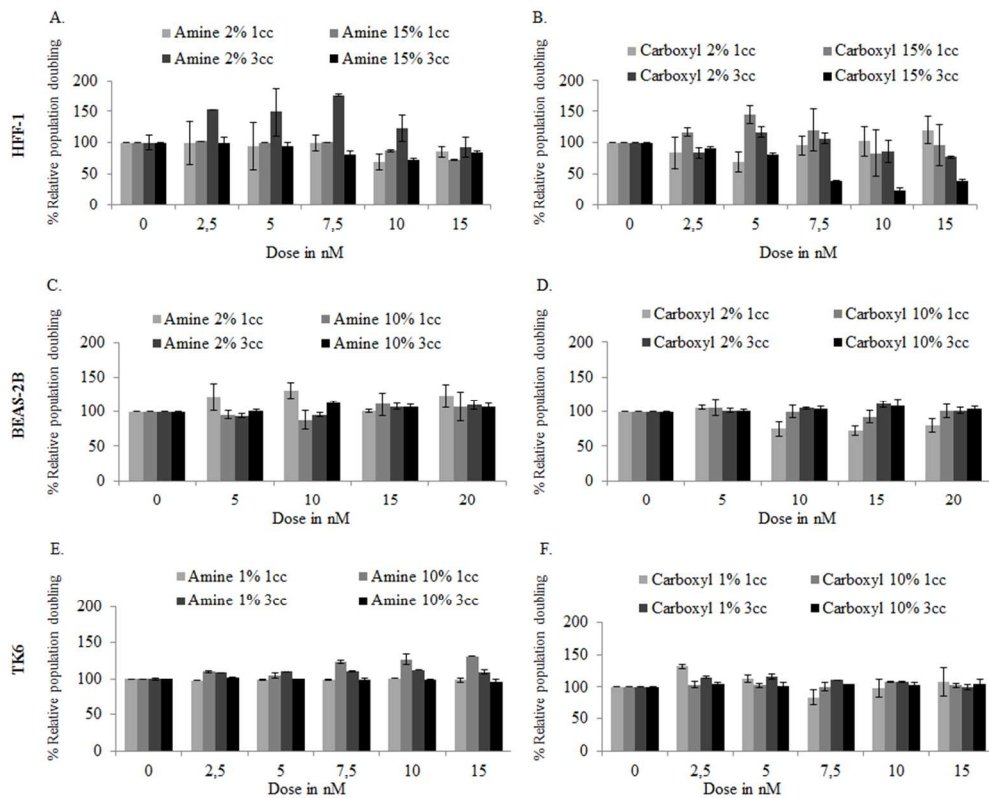
77x60mm (300 x 300 DPI)

1  
2  
3  
4  
5  
6  
7  
8  
9  
10  
11  
12  
13  
14  
15  
16  
17  
18  
19  
20  
21  
22  
23  
24  
25  
26  
27  
28  
29  
30  
31  
32  
33  
34  
35  
36  
37  
38  
39  
40  
41  
42  
43  
44  
45  
46  
47  
48  
49  
50  
51  
52  
53  
54  
55  
56  
57  
58  
59  
60

1  
2  
3  
4  
5  
6  
7  
8  
9  
10  
11  
12  
13  
14  
15  
16  
17  
18  
19  
20  
21  
22  
23  
24  
25  
26  
27  
28  
29  
30  
31  
32  
33  
34  
35  
36  
37  
38  
39  
40  
41  
42  
43  
44  
45  
46  
47  
48  
49  
50  
51  
52  
53  
54  
55  
56  
57  
58  
59  
60

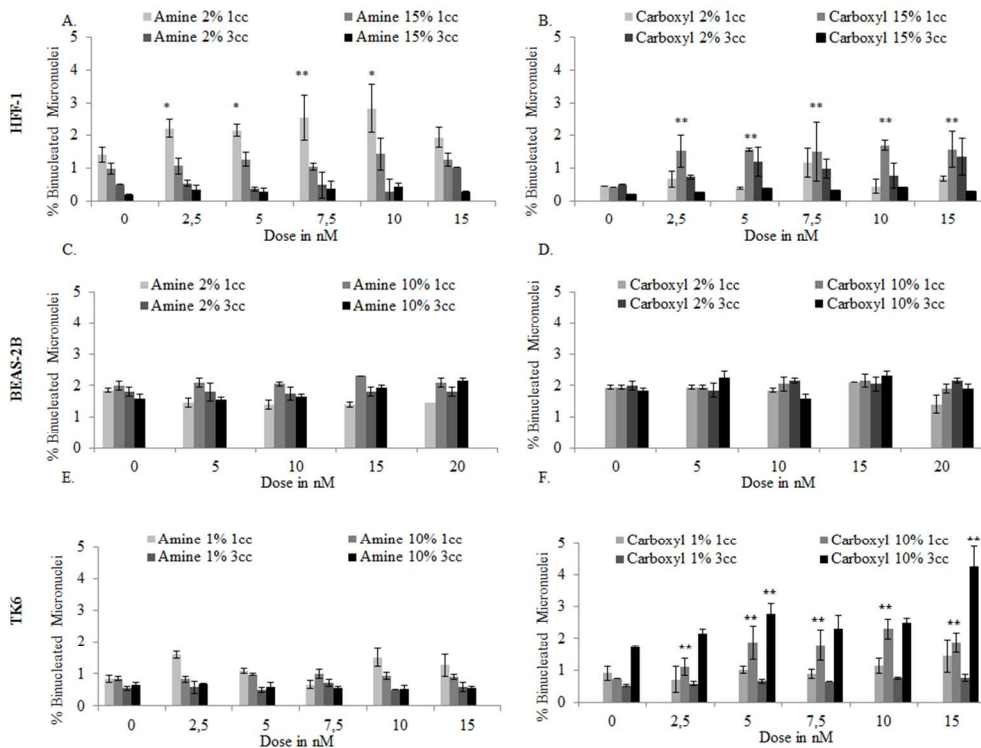


80x27mm (300 x 300 DPI)



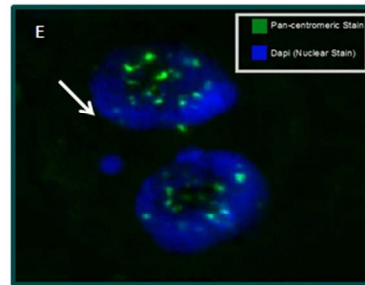
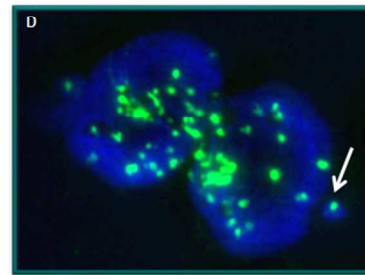
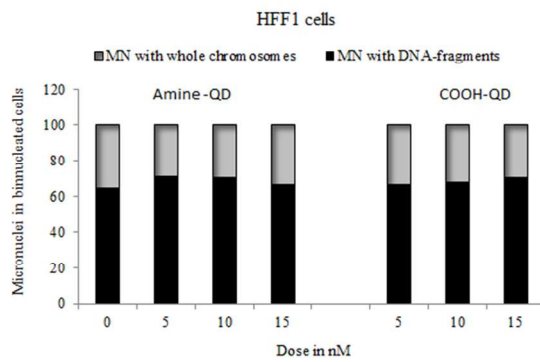
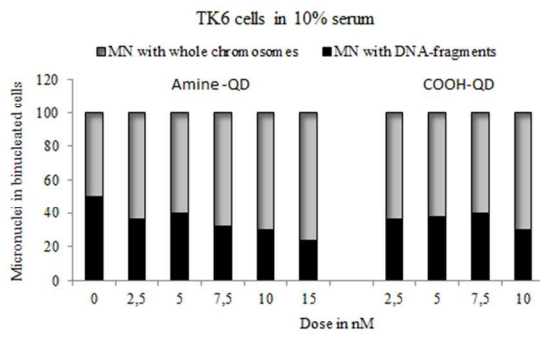
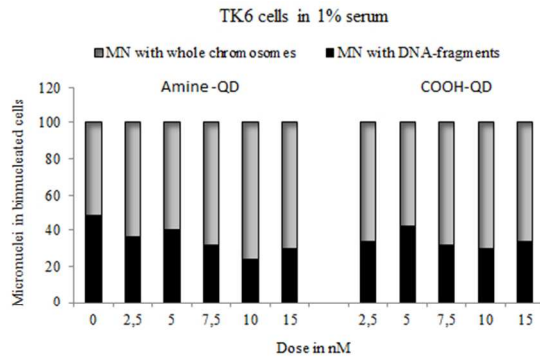
81x64mm (300 x 300 DPI)

1  
2  
3  
4  
5  
6  
7  
8  
9  
10  
11  
12  
13  
14  
15  
16  
17  
18  
19  
20  
21  
22  
23  
24  
25  
26  
27  
28  
29  
30  
31  
32  
33  
34  
35  
36  
37  
38  
39  
40  
41  
42  
43  
44  
45  
46  
47  
48  
49  
50  
51  
52  
53  
54  
55  
56  
57  
58  
59  
60



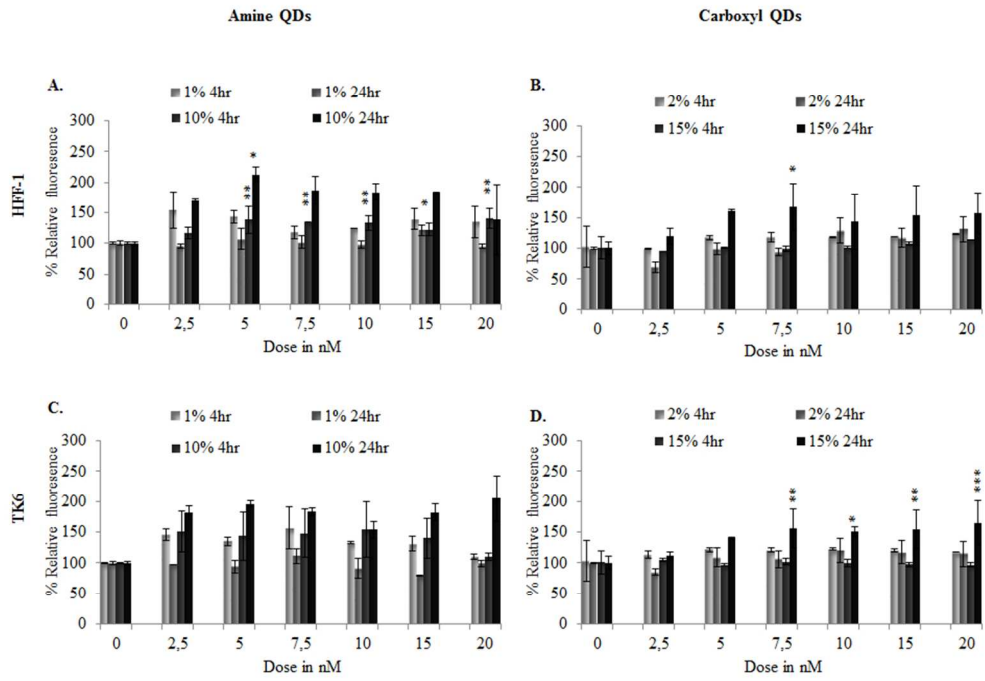
85x63mm (300 x 300 DPI)

1  
2  
3  
4  
5  
6  
7  
8  
9  
10  
11  
12  
13  
14  
15  
16  
17  
18  
19  
20  
21  
22  
23  
24  
25  
26  
27  
28  
29  
30  
31  
32  
33  
34  
35  
36  
37  
38  
39  
40  
41  
42  
43  
44  
45  
46  
47  
48  
49  
50  
51  
52  
53  
54  
55  
56  
57  
58  
59  
60



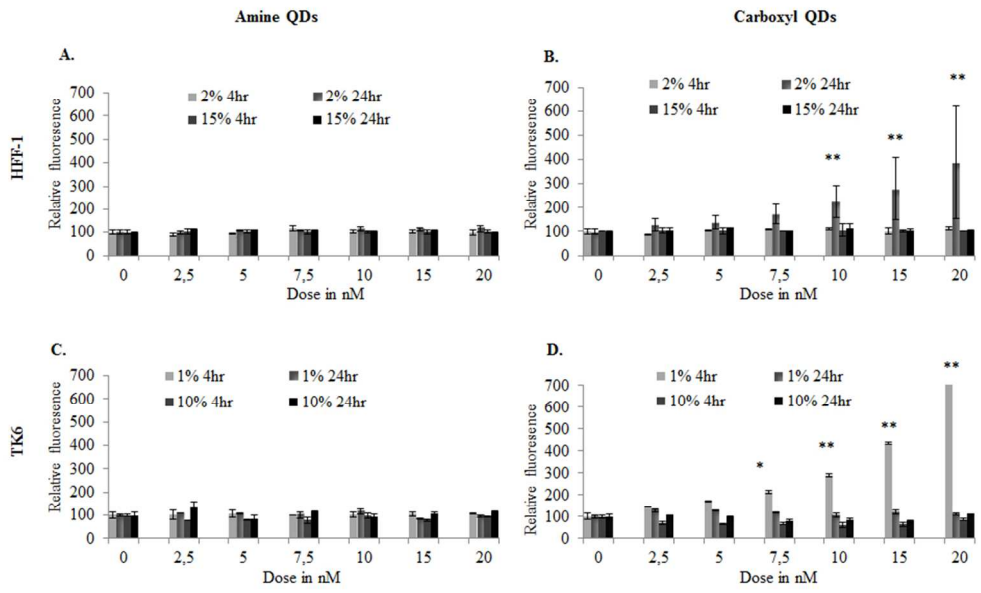
72x80mm (300 x 300 DPI)

1  
2  
3  
4  
5  
6  
7  
8  
9  
10  
11  
12  
13  
14  
15  
16  
17  
18  
19  
20  
21  
22  
23  
24  
25  
26  
27  
28  
29  
30  
31  
32  
33  
34  
35  
36  
37  
38  
39  
40  
41  
42  
43  
44  
45  
46  
47  
48  
49  
50  
51  
52  
53  
54  
55  
56  
57  
58  
59  
60



81x56mm (300 x 300 DPI)

1  
2  
3  
4  
5  
6  
7  
8  
9  
10  
11  
12  
13  
14  
15  
16  
17  
18  
19  
20  
21  
22  
23  
24  
25  
26  
27  
28  
29  
30  
31  
32  
33  
34  
35  
36  
37  
38  
39  
40  
41  
42  
43  
44  
45  
46  
47  
48  
49  
50  
51  
52  
53  
54  
55  
56  
57  
58  
59  
60



81x49mm (300 x 300 DPI)

1  
2  
3  
4  
5  
6  
7  
8  
9  
10  
11  
12  
13  
14  
15  
16  
17  
18  
19  
20  
21  
22  
23  
24  
25  
26  
27  
28  
29  
30  
31  
32  
33  
34  
35  
36  
37  
38  
39  
40  
41  
42  
43  
44  
45  
46  
47  
48  
49  
50  
51  
52  
53  
54  
55  
56  
57  
58  
59  
60